Supporting Information

Effect of Imidazole Arrangements on Proton-Conductivity in Metal-Organic Frameworks

Feng-Ming Zhang,[†,‡,¶] Long-Zhang Dong,[†,¶] Jun-Sheng Qin,[§,¶] Wei Guan,[⊥] Jiang Liu,[†] Shun-Li Li,[†] Meng Lu,[†] Ya-Qian Lan,*[,†] Zhong-Min Su,[⊥] and Hong-Cai Zhou*[,§]

[†] Jiangsu Collaborative Innovation Centre of Biomedical Functional Materials, Jiangsu Key Laboratory of New Power Batteries, School of Chemistry and Materials Science, Nanjing Normal University, Nanjing, 210023, P. R. China

[‡] College of Chemical and Environmental Engineering, Harbin University of Science and Technology, Harbin, 150040, P. R. China

[§] Department of Chemistry, Department of Materials Science and Engineering, Texas A&M Energy Institute, Texas A&M University, College Station, Texas 77843-3255, United States

[⊥] Department of Chemistry, Northeast Normal University, Changchun 130024, P. R. China

Table of Contents

S1 Materials and Synthetic Details

All solvents and reagents were analytical grade and used without further purification. Acetic acid (HAc), *N*,*N*-diethylformamide (DEF), imidazole, sodium acetate trihydrate ($CH_3COONa·3H_2O$), iron(III) nitrate nonahydrate ($Fe(NO)_3·9H_2O$), ferrous sulfate heptahydrate ($FeSO_4·7H_2O$), and [1,1′:3′,1″-terphenyl]-4,4″,5′-tricarboxylic acid (H_3L) were purchased from China National Medicines Corporation LTD. The cluster $[Fe^{III}_2Fe^{II}(\mu_3\text{-}O)(CH_3COO)_6(H_2O)_3]$ (abbreviated to $Fe_3O(CH_3CO_2)_6$) was prepared according to the reported method.[1] In detail, a aqueous solution (140 mL) containing sodium acetate trihydrate (82 g, 0.62 mol) was added into a water solution (140 mL) of $Fe(NO)_3·9H_2O$ (16.2 g, 0.04 mol) and $FeSO_4·7H_2O$ (5.6 g, 0.2 mol) with rapid stirring. Then the resulting precipitate was filtered and washed several times with water and ethanol.

Synthesis of Fe-MOF. $Fe_3O(CH_3CO_2)_6$ (15 mg) in 2 mL *N*,*N*-diethylformamide (DEF) was ultrasonically to dissolve, then ligand (15 mg) and acetic acid (0.30 mL) were added into the solution. This solution was transferred into a 15 mL Teflon-lined stainless steel autoclave for 32 h at 423 K under autogenous pressure. After cooling down to room temperature, brown crystals were collected by filtration and fully washed with DEF and methanol. The crystals were soaked in 20 mL of methanol for 3 days and CH_2Cl_2 for 3 days, respectively, then filtered and dried under vacuum. Yield: 65%. FT-IR (4000–400 cm^{-1}, see Figure S4): 3426 (m), 2980 (w), 1653 (s), 1607 (s), 1400 (s), 1259 (w), 1114 (w), 783 (m), 501 (w). Elemental analysis calcd. for $[Fe_3(\mu_3{-}O)(C_{21}H_{11}O_6)_2(H_2O)_3]$ ($C_{42}H_{28}Fe_3O_{16}$): C, 52.76; H, 2.95; N, 0.00. Found: C, 52.68; H, 3.03; N, 0.00.

Synthesis of Im@Fe-MOF. The activated sample of Fe-MOF was immerged in 1 M methanol solution of imidazole for three days. Then the crystals were filtered and dried under vacuum. FT-IR (4000–400 cm^{-1}): 3404 (m), 3140 (w), 1657 (m), 1598 (m), 1546 (m), 1400 (s), 1178 (w), 1104 (w), 1053 (w), 1009 (w), 854 (w), 774 (m), 501 (w). Elemental analysis found: C, 55.17; H, 3.22; N, 8.71.

Synthesis of Im-Fe-MOF. $Fe_3O(CH_3CO_2)_6$ (15 mg) in 2 mL DEF was ultrasonically to dissolve, then ligands (15 mg), imidazole (15 mg) and acetic acid (0.35 mL) were added into the solution. This solution was transferred into a 15 ml Teflon-lined stainless steel autoclave for 18 h at 423 K under autogenous pressure. After cooling down to room temperature, dark brown crystals were collected by filtration and fully washed with DEF and methanol. The crystals were soaked in 20 mL of methanol for 3 days and CH_2Cl_2 for 3 days, respectively, then filtered and dried under vacuum. Yield: 60%. FT-IR (4000–400 cm^{-1}): 3426 (m), 3140 (w), 2987 (w), 2933 (w), 1650 (s), 1592 (s), 1400 (s), 1261 (w), 1207 (w), 1107 (w), 1053 (w), 1006 (w), 945 (w), 867 (w), 783 (m), 621 (w) 506 (w). Elemental analysis calcd. for $[Fe_3(\mu_3{-}O)(C_{21}H_{11}O_6)_2(C_3N_2H_4)_3]$ ($C_{51}H_{34}Fe_3N_6O_{13}$): C, 55.36; H, 3.10; N, 7.60. Found: C, 55.28; H,

3.13; N, 7.65.

Instrumentation. Infrared spectrum using the KBr pellet was measured on a Bruker Tensor 27 in the range of 4000-400 cm^{-1}. Thermogravimetric (TG) analysis was carried out on a Netzch STA449F3 analyser at a heating rate of 10 °C/min from ambient temperature to 700 °C. Elemental analysis (EA) were conducted using an Elementar vario EL III analyzer. The room temperature powder X-ray diffraction (PXRD) spectra were recorded on a Rigaku D/Max 2500/PC diffractometer at 40 kV, 100 mA with a Cu-target tube and a graphite monochromator. X-ray photoelectron spectroscopy (XPS) was used a K-Alpha instrument from Thermo Scientific equipped with an Al Kα microfocused X-ray source and the C_{1s} peak at 284.6 eV as internal standard The as−synthesized samples were used to XPS measurement without activation and the sample of Im@Fe−MOF was prepared in DEF solution of imidazole. Nitrogen adsorption-desorption isotherms were measured at 77 K on a Autosorb IQ2 adsorptometer (Quantachrome Instruments), and water vapor adsorption isotherms were measured at 298 K.

X-ray crystallography. The single-crystal diffraction data for Fe-MOF and Im-Fe-MOF were collected on D8 Venture PHOTON 100 CMOS diffractometer at 173 K and Bruker AXS smart Apex CCD diffractometer at 100 K, respectively. The X-ray generator was operated at 50 kV and 35 mA using Mo-Kα (λ = 0.71073 Å) radiation. The crystal structures were solved and refined by full matrix least-squares methods against F^2 using the SHELXL-2014[2] program package and Olex-2 software.[3] All non-hydrogen atoms were refined with anisotropic displacement parameters and hydrogen positions were fixed at calculated positions and refined isotropically. The solvent molecules in these structures are highly disordered and not able to be refined by using conventional discrete-atom models; thus, the contribution of partial solvent electron densities was removed by the SQUEEZE routine in PLATON.[4]The topological analyses were performed with TOPOS.[5] The crystallographic data and structure refinement for Fe-MOF and Im-Fe-MOF are summarized in Table S2. The selected bond lengths and angles of Fe-MOF and Im-Fe-MOF are listed in Tables S3−4. CCDC 1504095 (for Fe-MOF) and 1504094 (for Im-Fe-MOF) contain the supplementary crystallographic data for this paper. These data can be obtained free of charge from The Cambridge Crystallographic Data Centre.

Impedance analysis. The samples were put into a homemade mould with a radius of 0.2 cm to get circular pellets. The thickness was measured by a vernier caliper. And then the pellets were smeared by silver colloid on two sides which were fixed on the sample stage with gold wires. The proton conductivities were measured using an impedance/gain-phase analyzer (Solartron S1 1260) over a frequency range from 1 Hz to 1 MHz with an input voltage range from 100 mV to 3000 mV. The measurements were operated at temperatures (25 to 60 °C), with different relative humidities (40% to 98%RH). The proton conductivity was calculated

using the following equation

$$\sigma = \frac{l}{SR}$$

where σ is the conductivity (S cm^{-1}), l is the thickness (cm) of the pellet, S is the cross-sectional area (cm^2) of the pellet and R is the bulk resistance (Ω). The activation energy (E_a) was calculated from the following equation

$$\ln \sigma_T = \ln \sigma_0 - \frac{E_a}{KT} \qquad (K = 8.6\times10^{-5}\ \text{eV/K})$$

where σ is the conductivity (S cm^{-1}), K is the Boltzmann constant (eV/K) and T is the temperature (K).

Computational Details. Two simplified model structures $Fe_3(\mu_3\text{-}O)(C_6H_5COO)_6(H_2O)_3$ and $Fe_3(\mu_3\text{-}O)(C_6H_5COO)_6(C_3H_4N_2)_3$ of were extracted from crystal structures of Fe-MOF and Im-Fe-MOF, respectively. All geometries were optimized with a spin-unrestricted broken-symmetry strategy at the level of the UB3LYP hybrid functional in the gas phase.[6] The LANL2DZ basis set was employed for the Fe with Los Alamos relativistic effective core potentials (ECPs),[7] while the 6-31G(d) basis set was used for the other main-group elements. All single-point calculations were performed using a spin-unrestricted broken-symmetry UB3LYP functional with both the Stuttgart/Dresden ECP basis sets (SDD)[8] and 6-311++G(d,p) basis sets. The solvent effect of water was evaluated by the conductor-like polarizable continuum model (CPCM).[9]

The binding energies of H(-OH) and H($-N_2C_3H_3$) with the rest of Fe-MOF and Im-Fe-MOF were calculated at the B3LYP/[6-31G(d)/LANL2DZ(Fe)] level, respectively, as the following formula.

$E_b = E_1 - E_{2-H} - E_H - E_{BSSE}$

where E_b is the binding energies, E_1 is defined as the energy of complex $Fe_3(\mu_3\text{-}O)(C_6H_5COO)_6(H_2O)_3$, $E_{\mathbf{1\text{-}H}}$ is the energy of the $Fe_3(\mu_3\text{-}O)(C_6H_5COO)_6(H_2O)_2(HO)$ moiety in $Fe_3(\mu_3\text{-}O)(C_6H_5COO)_6(H_2O)_3$, $E_{\mathbf{H}}$ denotes the energy of the corresponding H in $Fe_3(\mu_3\text{-}O)(C_6H_5COO)_6(H_2O)_3$, and E_{BSSE} is the energy of basis set superposition error, respectively. A similar methodology ($E_b = E_2 - E_{2-H} - E_H - E_{BSSE}$) was employed to $Fe_3(\mu_3\text{-}O)(C_6H_5COO)_6(C_3H_4N_2)_3$ discussed in the text.

All of these calculations were performed by the Gaussian 09 program package.[10]

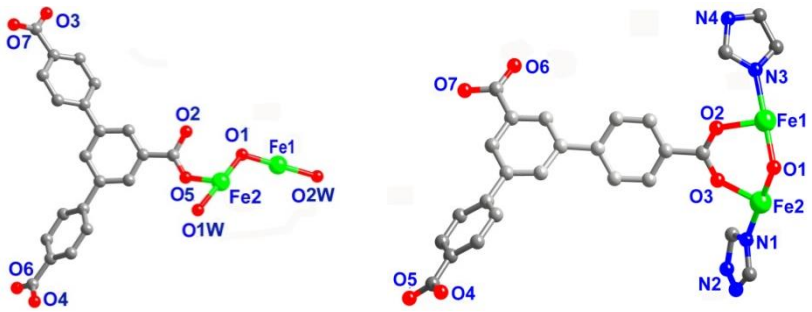

Figure S1. Asymmetric units of the Fe−MOF (*left*) and Im−Fe−MOF (*right*).

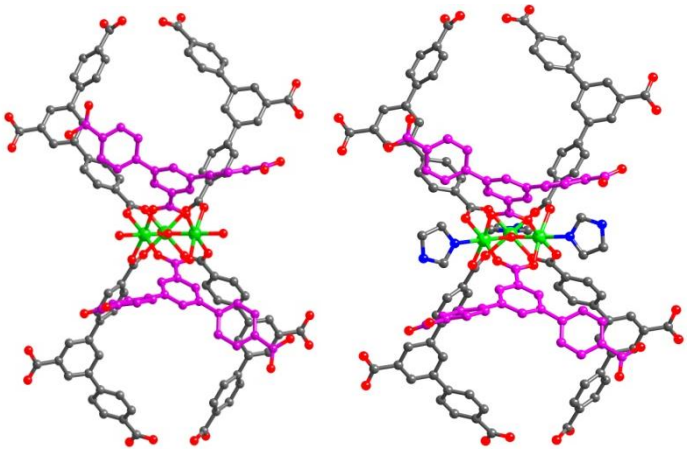

Figure S2. Trinuclear metal clusters coordinated by six ligands in Fe-MOF (*left*) and Im-Fe-MOF (*right*), respectively.

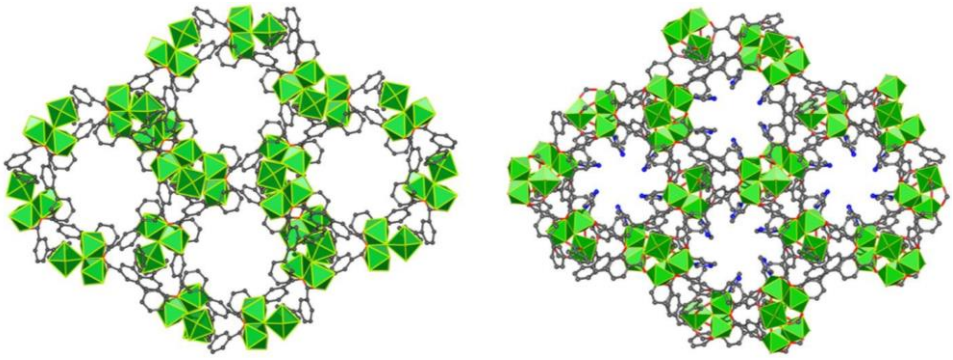

Figure S3. Structures of Fe-MOF (*left*) and Im-Fe-MOF (*right*) viewed in the direction of *c*-axis.

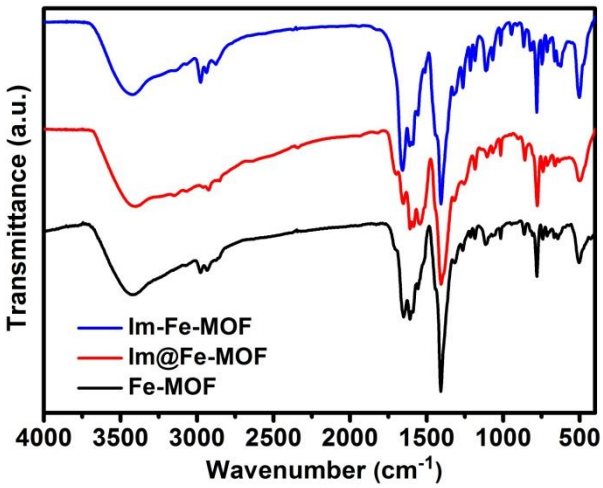

Figure S4. IR spectra of Fe-MOF, Im@Fe-MOF and Im-Fe-MOF.

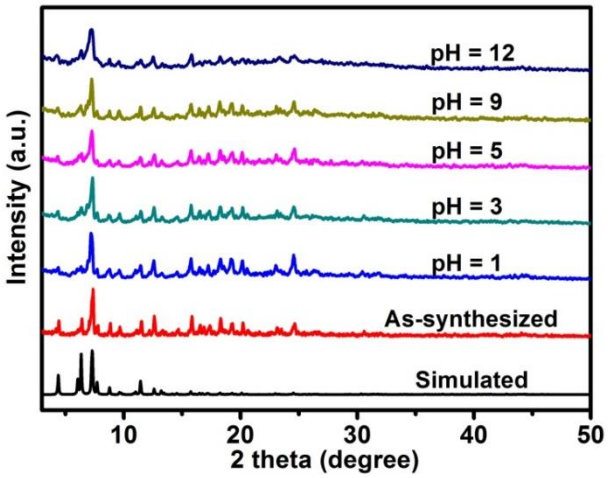

Figure S5. PXRD patterns of Fe-MOF for the simulated pattern, as-synthesized, and samples at indicated pH values.

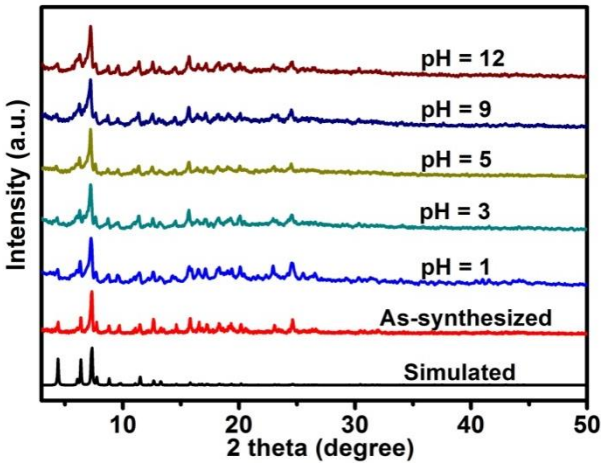

Figure S6. PXRD patterns of Im-Fe-MOF for the simulated, as-synthesized, and samples at indicated pH values.

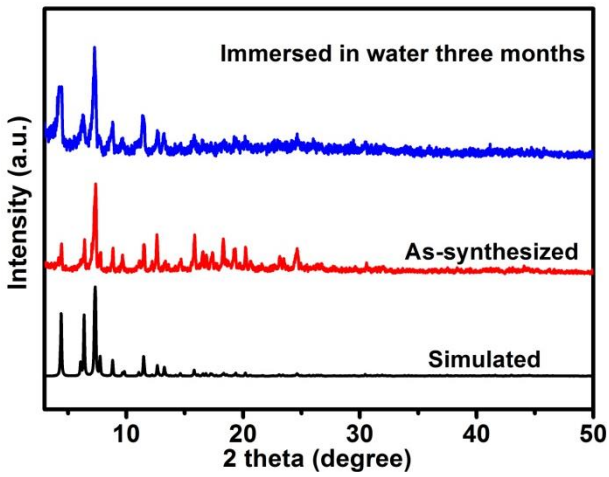

Figure S7. PXRD patterns of Im-Fe-MOF for the simulated one, as-synthesized sample and sample immersed in water for three months.

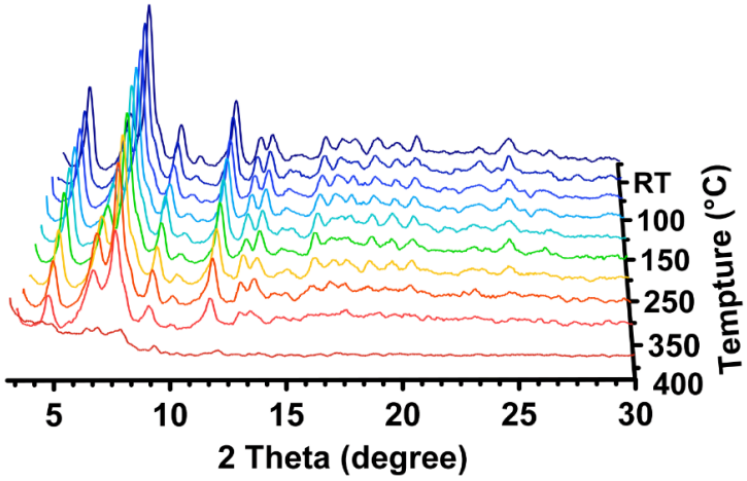

Figure S8. Variable temperature PXRD patterns of Fe−MOF.

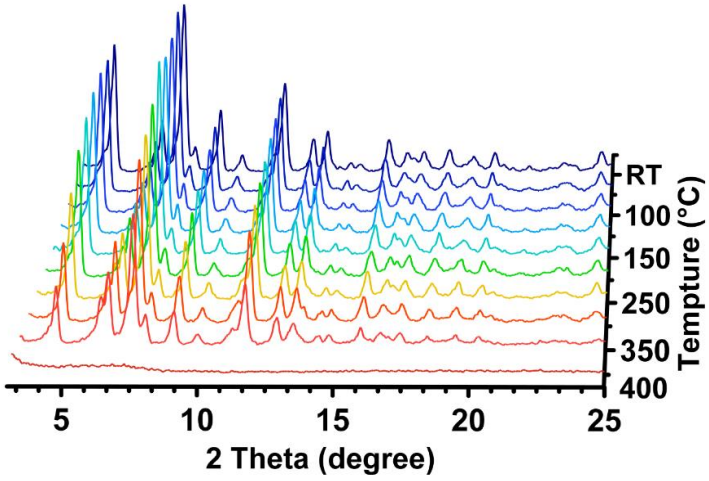

Figure S9. Variable temperature PXRD patterns of Im−Fe−MOF.

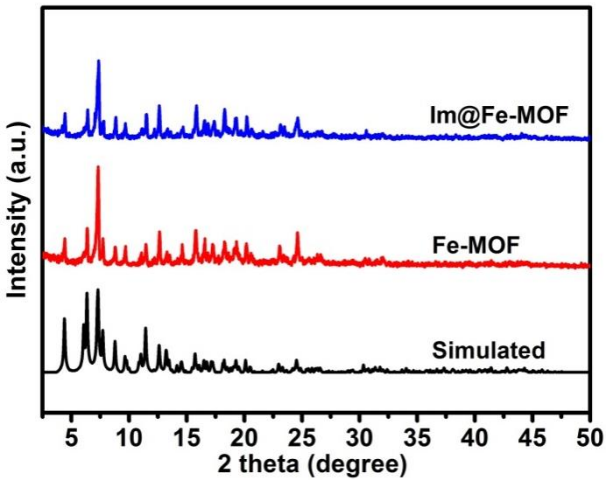

Figure S10. PXRD patterns of Im@Fe-MOF, Fe-MOF and the simulated one.

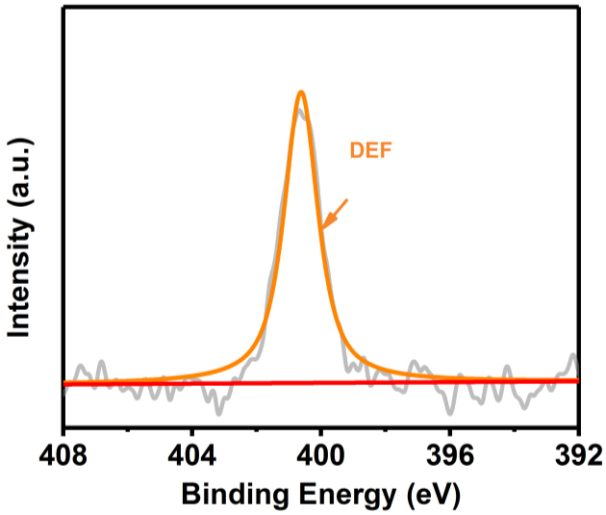

Figure S11. Nitrogen 1s photoelectron spectrum for Fe−MOF.

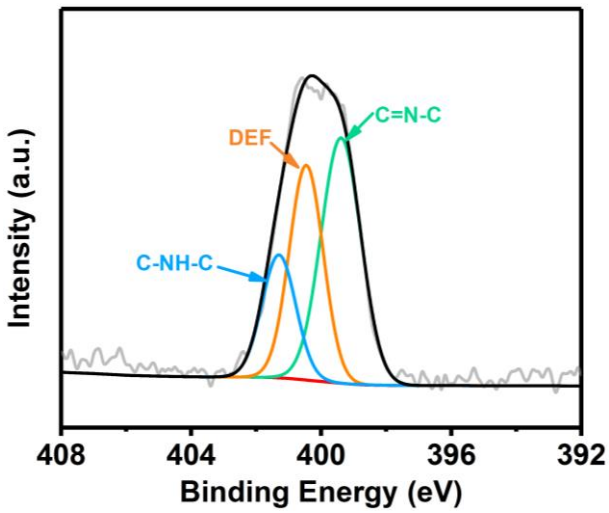

Figure S12. Nitrogen 1s photoelectron spectrum for Im@Fe−MOF.

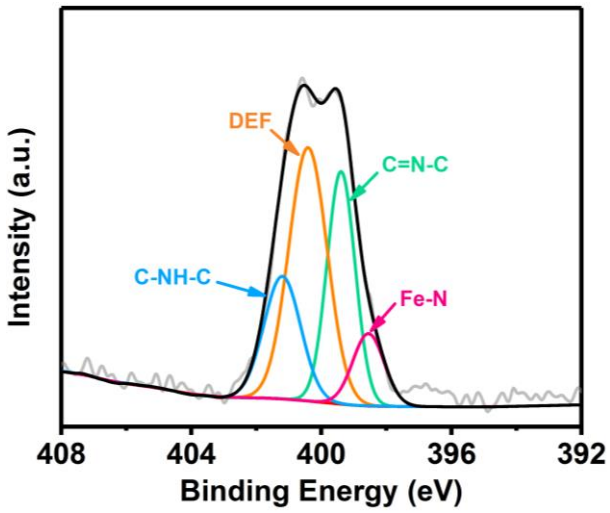

Figure S13. Nitrogen 1s photoelectron spectrum for Im−Fe−MOF.

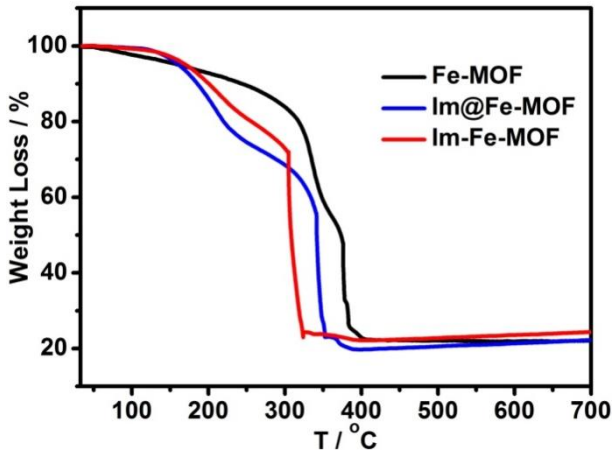

Figure S14. Thermogravimetric analyses of Fe-MOF, Im@Fe-MOF and Im-Fe-MOF.

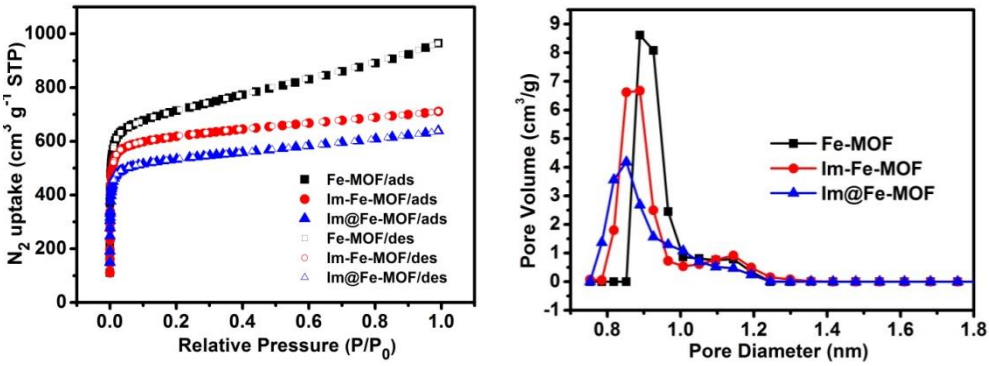

Figure S15. Nitrogen gas adsorption and desorption isotherms at 77 K (*left*) and pore size distribution profiles (*right*) for Fe-MOF, Im-Fe-MOF and Im@Fe-MOF, respectively.

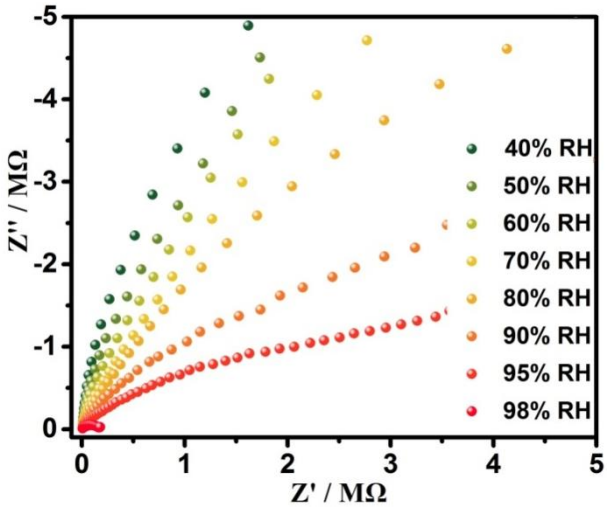

Figure S16. Impedance spectra of Fe-MOF at 25 °C with different RHs.

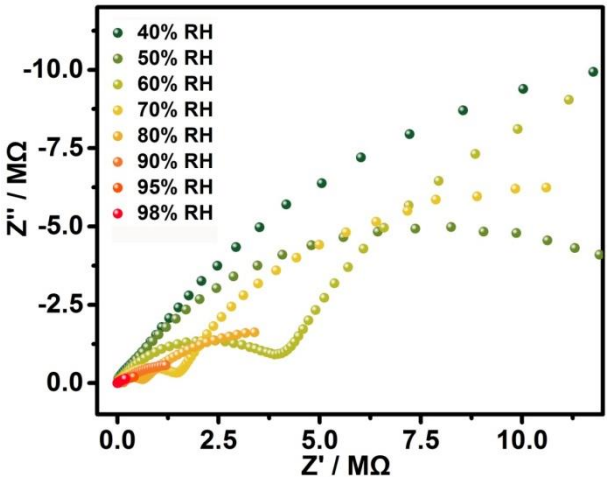

Figure S17. Impedance spectra of Im@Fe-MOF at 25 °C with different RHs.

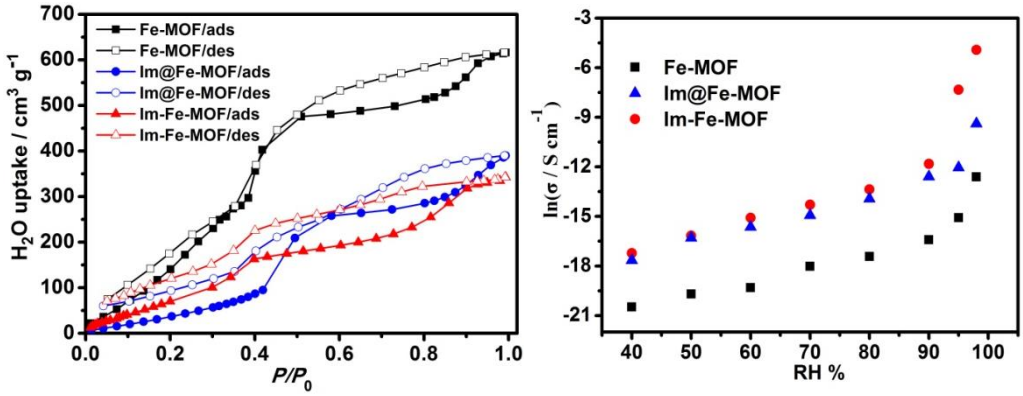

Figure S18. Water vapor adsorption and desorption isotherms (*left*), and humidity dependence of conductivities at 25 °C (*right*) for Fe-MOF, Im@Fe-MOF and Im-Fe-MOF.

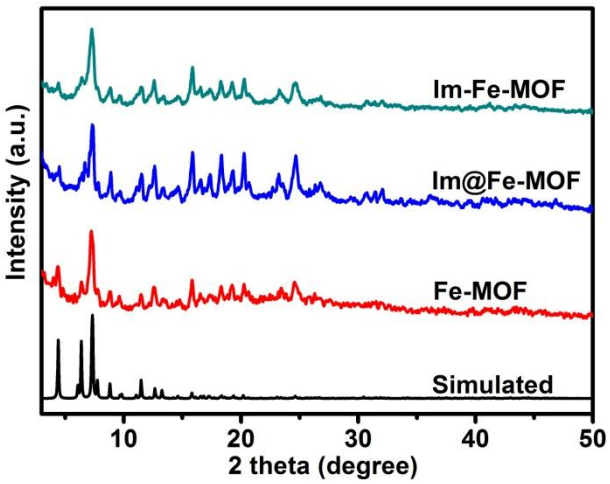

Figure S19. PXRD patterns of Fe-MOF, Im@Fe-MOF and Im-Fe-MOF after water-vapor adsorption.

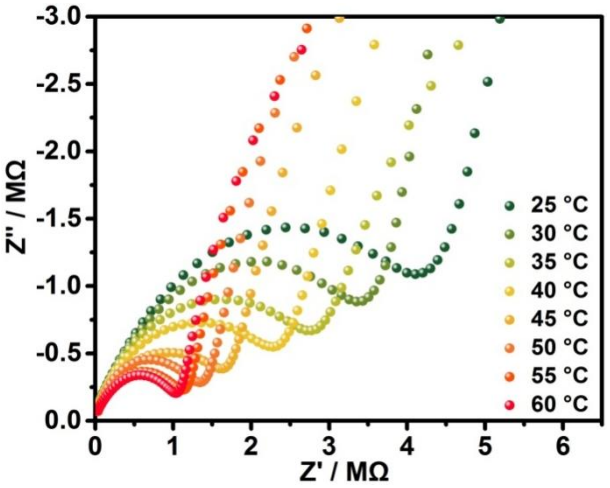

Figure S20. Impedance spectra of Fe-MOF under 80% RH with different temperatures.

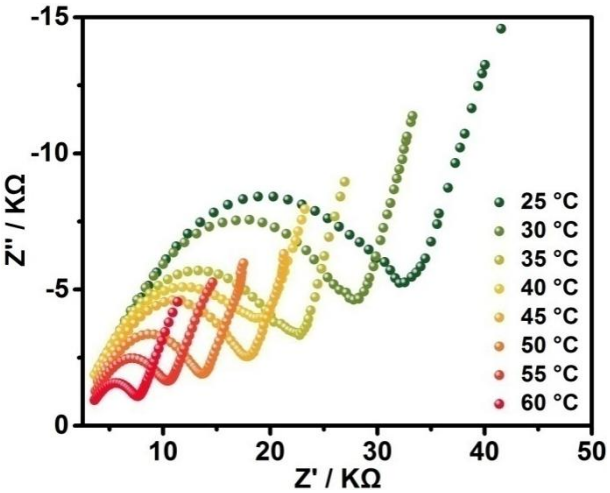

Figure S21. Impedance spectra of Fe-MOF under 98% RH with different temperatures.

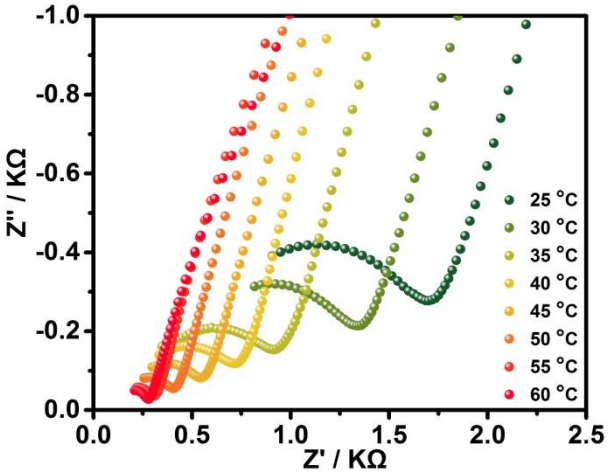

Figure S22. Impedance spectra of Im@Fe-MOF under 98% RH with different temperatures.

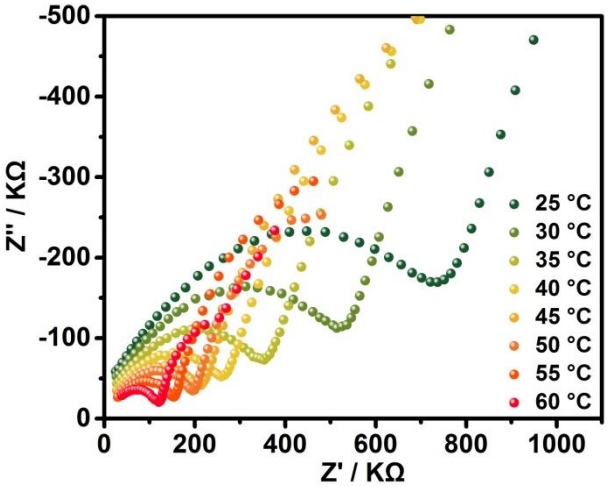

Figure S23. Impedance spectra of Im-Fe-MOF under 80% RH with different temperatures.

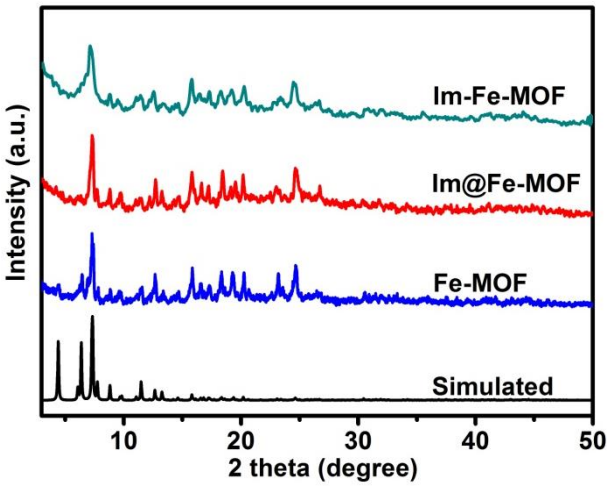

Figure S24. PXRD patterns of Fe-MOF, Im@Fe-MOF and Im-Fe-MOF after impedance analysis.

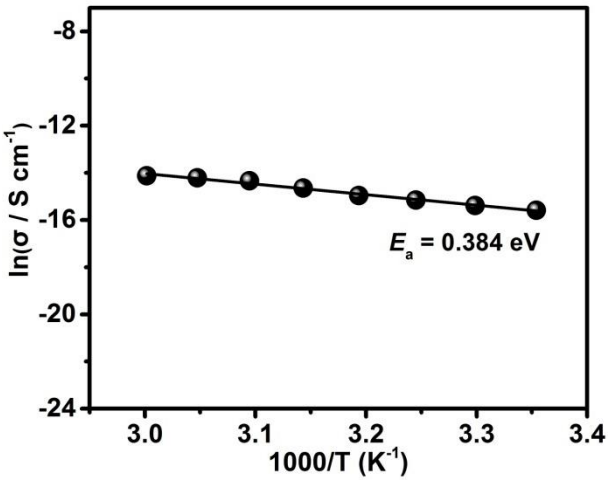

Figure S25. Arrhenius plots of the proton conductivities for Fe-MOF under 80% RH.

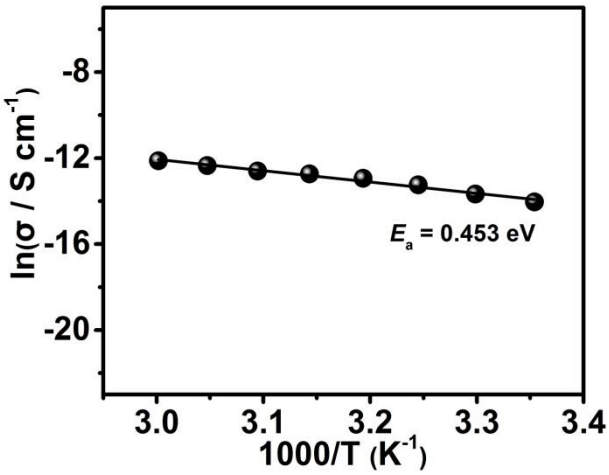

Figure S26. Arrhenius plots of the proton conductivities for Im-Fe-MOF under 80% RH.

Table S1. Comparison of proton conductivity of Im-Fe-MOF with some other representative proton conductors measured under hydrous condition.

Compounds	**σ (S cm^{-1})**	**E_a (eV)**	**Reference**
Im-Fe-MOF	1.21×10^{-2} (60°C, 98%RH)	0.436	This work
Nafion	5×10^{-2} (30°C, 98%RH)	0.22	11
$Fe(ox)\cdot2H_2O$	3.23×10^{-3} (45°C, 98%RH)	0.37	12
PCMOF-3	3.5×10^{-5} (25°C, 98%RH)	0.17	13
$(NH_4)_4[MnCr_2(ox)_6]\cdot4H_2O$	1.7×10^{-3} (40°C, 96%RH)	0.23	14
$Fe(OH)(bdc\text{-}(COOH)_2)$	7×10^{-6} (80°C, 95%RH)	0.21	15
$Cu_3Mo_5P_2$	2.2×10^{-5} (28°C, 98%RH)	0.232	16
$\{NMe_3(CH_2COOH)\}[FeCr(ox)_3]\cdot nH_2O$	0.8×10^{-4} (25°C, 65%RH)	/	17
$\{NEt_3(CH_2COOH)\}[MnCr(ox)_3]\cdot nH_2O$	2×10^{-4} (25°C, 80%RH)	/	17
$\{NBu_3(CH_2COOH)\}[MnCr(ox)_3]\cdot nH_2O$	5×10^{-6} (25°C, 90%RH)	/	17
$\{NBu_3(CH_2COOH)\}[FeCr(ox)_3]\cdot nH_2O$	0.9×10^{-7} (25°C, 90%RH)	/	17
Ca-SBBA	8.58×10^{-6} (25°C, 98%RH)	0.23	18
Sr-SBBA	4.4×10^{-5} (25°C, 98%RH)	0.56	18
In-IA-2D-1	3.4×10^{-3} (27°C, 98%RH)	0.61	19
In-IA-2D-2	4.2×10^{-4} (27°C, 98%RH)	0.48	19
PCMOF-5	2.51×10^{-3} (60°C, 98%RH)	0.16	20
$\{H[Cu(Hbpdc(H_2O)_2]_2[PMo_{12}O_{40}]\cdot nH_2O\}_n$	1.25×10^{-3} (100°C, 98%RH	1.02	21
$\{H[Cu(Hbpdc(H_2O)_2]_2[PW_{12}O_{40}]\cdot nH_2O\}_n$	156×10^{-3} (100°C, 98%RH)	1.02	21
$\{[Ca(D\text{-}Hpmpc)(H_2O)_2]\cdot2HO_{0.5}\}_n$	8.9×10^{-4} (60°C, 97%RH)	0.21	22
$\{H[Ni(Hbpdc)(H_2O)_2]_2[PW_{12}O_{40}]\cdot8H_2O$	1.35×10^{-3} (100°C, 98%RH)	1.01	23
$\{[H_3O][Cu_2(DSOA)(OH)(H_2O)]\cdot9.5H_2O\}_n$	1.9×10^{-3} (85°C, 98%RH)	1.04	24
PCMOF2½	2.1×10^{-2} (85°C, 90%RH)	0.21	25
$\{[(Me_2NH_2)_3(SO_4)]_2[Zn(ox)_3]\}_n$	4.2×10^{-2} (25°C, 98%RH)	0.129	26
EuL	1.6×10^{-5} (75°C, 97%RH)	0.91	27
DyL	1.33×10^{-5} (75°C, 97%RH)	0.87	27
HKUST-1	1.08×10^{-8} (90°C, 70%RH)	0.69	28
NENU-3	4.76×10^{-5} (90°C, 70%RH)	0.41	28
NENU-3-Ina	1.81×10^{-3} (90°C, 70%RH)	0.36	28
$(NH_4)_2(adp)[Zn_2(ox)_3]\cdot2H_2O$	7×10^{-5} (25°C, 100%RH)	/	29
$(NH_4)_2(adp)[Zn_2(ox)_3]\cdot3H_2O$	8×10^{-3} (25°C, 100%RH)	/	29
$H^+@Ni_2(dobdc)$ pH=1.8	2.2×10^{-2} (80°C, 95%RH)	0.12	30

$\{[Cu_3(L)_2(H_2O)_4][Cu(dmf)_4(SiW_{12}O_{40})]\cdot 9H_2O$	5.94×10^{-4}(100°C, 98%RH)	0.32	31
$[H_3O][CoLa(notp)(H_2O)_4]ClO_4\cdot 3H_2O$	4.24×10^{-5} (25°C, 98%RH）	0.28	32
$[Cu_3(u_3\text{-}OH)(H_2O)_3(atz)_3]_3[P_2W_{18}O_{62}]\cdot 14H$	4.4×10^{-6} (25°C, 97%RH)	/	33
$[Cu(H_2L)(DMF)_4]_n$	3.46×10^{-3} (95°C, 95%RH)	0.68	34
$[CaL_{0.5}(DMF)_{2.5}]_n$	1.27×10^{-5} (25°C, 95%RH)	0.17	34
$[CdL_{0.5}(DMF)_2]_n$	2.49×10^{-7} (25°C, 95%RH)	0.59	34
$[Cd_2(btc)_2(H_2O)_2]_n\cdot n(H_2bmib)\cdot 6n(H_2O)$	5.4×10^{-5} (60°C, 95%RH)	0.62	35
$[Cd_4(cpip)_2(Hcpip)_2]_n\cdot n(H_2bmib)\cdot n(H_2O)$	2.2×10^{-5} (60°C, 95%RH)	0.27	35
ZIF-8	4.6×10^{-4} (94°C, 98%RH)	/	36
PCMOF10	3.55×10^{-2} (70°C, 95%RH)	0.4	37
$\{[Zn(C_{10}H_2O_8)_{0.5}(C_{10}S_2N_2H_8)]\cdot 5H_2O]\}_n$	2.55×10^{-7} (80°C, 95%RH)	0.96	38
$\{[Zn(C_{10}H_2O_8)_{0.5}(C_{10}S_2N_2H_8)]\cdot 2H_2O]\}_n$	4.39×10^{-4} (80°C,95%RH)	0.84	38
$Cu_4(L)_2(OH)_2(DMF)_2$	7.4×10^{-4} (95°C, 95%RH)	1.32	39
$UiO\text{-}66(SO_3H)_2$	8.4×10^{-2} (80°C, 90%RH)	0.32	40
$UiO\text{-}66(Zr)\text{-}(CO_2H)_2$	2.3×10^{-3} (90°C, 95%RH)	0.17	41
$[Cu_3(BTC)_2(H_2O)_3]_4[SiW_{11}Mo^{v}O_{40}](C_4H_{12}N_5)$	6.37×10^{-8} (25°C, 97%RH)	/	42
VNU-15	2.90×10^{-2} (95°C, 60%RH)	0.22	43
MFM-500 (Ni)	4.5×10^{-4} (25°C, 98%RH)	0.43	44
Fe-CAT-5	5.0×10^{-2} (25°C, 98%RH)	0.24	45
Ti-CAT-5	8.2×10^{-4} (25°C, 98%RH)	0.43	45

Im = Imidazole, ox = oxalate, PCMOF-3 = $Zn_3(L)(H_2O)_2\cdot 2H_2O$ (L = 1,3,5-benzenetriphosphonate), H_2bdc = 1,4-benzenedicarboxylic acid, In-IA-2D-1 = $[In(IA)_2\{(CH_3)_2NH_2\}(H_2O)_2]$ In-IA-2D-2 = $[In(IA)_2\{(CH_3)_2NH_2\}(DMF)]$ (IA = isophthalic acid), PCMOF-5 = $LaH_5L(H_2O)_4$ (L = Benzene-1,2,4,5-tetramethylenephosphonic acid), H_2bpd = 2,2′-bipyridyl-3,3′-dicarboxylic acid, D-H_2pmpc = D-1-(phosphonomethyl)piperdine-3-carboxylic acid, Na_2H_2DSOA = disodium-2,2′-disulfonate-4,4′-oxydibenzoic acid, adp = adipic acid, $dobdc^{4-}$ = 2,5-dioxido-1,4-benzenedicarboxylate, $notpH_6$ = $C_9H_{18}N_3(PO_3H_2)_3$, Hatz = 3-amino-1,2,4,triazolate, H_3btc = 1,3,5-benzenetricarboxylic acid, H_3cpip = 5-(4-carboxyphenoxy)isophthalic acid, PCMOF10 = $Mg_2(H_2O)_4(H_2L)\cdot H_2O$ (H_6L = 2,5-dicarboxy-1,4-benzenediphosphonic acid), BTC = 1,3,5-benzenetricarboxylate, VNU-15 = $Fe_4(BDC)_2(NDC)(SO_4)_4(DMA)_4$ (BDC = benzene-1,4-dicarboxylate, NDC = naphthalene-2,6-dicarboxylate), MFM-500(Ni) = $[M_3(H_3L)_2(H_2O)_9(C_2H_6SO)_3]$ (M = Ni, H_6L = benzene-1,3,5-p-phenylphosphonic acid), Fe-CAT-5 = $Fe(THO)\cdot Fe(SO_4)(DMA)_3$ (THO^{6-} = triphenylene-2,3,6,7,10,11-hexakis(olate)), Ti-CAT-5 = $Ti(THO)\cdot(DMA)_2$.

Table S2. Crystal data and structure refinement for Fe−MOF and Im−Fe−MOF

Complexes	**Fe−MOF**	**Im−Fe−MOF**
formula	$C_{42}H_{28}Fe_3O_{16}$	$C_{51}H_{34}Fe_3N_6O_{13}$
fw	956.19	1106.39
crystal system	trigonal	trigonal
space group	$R\bar{3}c$	$R\bar{3}c$
a (Å)	27.739(4)	27.696(5)
b (Å)	27.739	27.696
c (Å)	72.055(10)	72.829(13)
α (deg)	90	90
β (deg)	90	90
γ (deg)	120	120
V (Å^3)	48016(14)	48382(20)
Z	18	18
D_{calcd} (g cm^{-3})	0.595	0.684
R(int)	0.1381	0.0797
μ (mm^{-1})	0.431	0.432
F (000)	8748	10152
R_1 [$I > 2\sigma(I)$]^a	0.0966	0.0991
wR_2 [$I > 2\sigma(I)$]^b	0.2395	0.2242
R_1 (all data)	0.1454	0.1210
wR_2 (all date)	0.2645	0.2382
GOF on F^2	1.073	1.125

$^a R_1 = \sum||F_o| - |F_c||/|F_o|$. $^b wR_2 = [\sum w (F_o^2 - F_c^2)^2/\sum w(F_o^2)^2]^{1/2}$.

Table S3. Selected bond lengths (Å) and angles (deg) for Fe−MOF

Fe(1)−O(6)#1	1.979(4)	O(1)−Fe(1)−O(7)#4	95.39(11)
Fe(1)−O(1)	1.893(5)	O(1)−Fe(1)−O(2W)	180.0
Fe(1)−O(7)#3	2.003(4)	O(7)#4−Fe(1)−O(7)#3	169.2(2)
Fe(1)−O(2W)	2.070(6)	O(7)#4−Fe(1)−O(2W)	84.61(11)
Fe(2)−O(1W)	2.061(4)	O(1W)−Fe(2)−O(4)#2	83.49(16)
Fe(2)−O(1)	1.902(2)	O(1)−Fe(2)−O(1W)	178.60(15)
Fe(2)−O(5)	2.023(4)	O(1)−Fe(2)−O(5)	94.64(13)
Fe(2)−O(4)#2	2.063(3)	O(1)−Fe(2)−O(4)#2	97.89(15)
Fe(2)−O(2)#5	2.046(3)	O(1)−Fe(2)−O(2)#5	94.19(14)
Fe(2)−O(3)#4	2.031(4)	O(1)−Fe(2)−O(3)#4	94.95(13)
O(4)−Fe(2)#6	2.063(3)	O(5)−Fe(2)−O(1W)^2	85.66(16)
O(7)−Fe(1)#7	2.003(4)	O(5)−Fe(2)−O(4)#2	88.76(16)
O(6)#2−Fe(1)−O(6)#1	171.8(3)	O(5)−Fe(2)−O(2)#5	89.75(16)
O(6)#2−Fe(1)−O(7)#4	90.48(17)	O(5)−Fe(2)−O(3)#4	170.40(15)
O(6)#1−Fe(1)−O(7)#4	88.75(17)	O(2)#5−Fe(2)−O(1W)	84.44(15)
O(6)#2−Fe(1)−O(2W)	85.91(13)	O(2)#5−Fe(2)−O(4)#2	167.91(15)
O(6)#1−Fe(1)−O(2W)	85.91(13)	O(3)#4−Fe(2)−O(1W)	84.74(16)
O(1)−Fe(1)−O(6)#1	94.09(13)	O(3)#4−Fe(2)−O(4)#2	90.26(16)

Symmetry transformations used to generate equivalent atoms: #1 = – y + 1/3, – x + 2/3, z + 1/6; #2 = y + 1, – x + y + 1, – z; #3 = – y, x – y – 1, z; #4 = y + 4/3, x – 1/3, – z + 1/6; #5 = –

x + 4/3, – x + y + 2/3, – z + 1/6; #6 = x – y, x – 1, – z; #7 = –x + y + 1, – x, z.

Table S4. Selected bond lengths (Å) and angles (deg) for Im−Fe−MOF

Fe(1)−O(1)	1.914(3)	O(5)#1−Fe(1)−O(2)	90.93(17)
Fe(1)−O(2)	2.040(4)	O(5)#1−Fe(1)−O(6)#2	171.18(18)
Fe(1)−O(5)#1	2.016(4)	O(5)#1−Fe(1)−O(7)#3	90.05(18)
Fe(1)−O(6)#2	2.017(4)	O(5)#1−Fe(1)−N(3)	85.4(2)
Fe(1)−O(7)#3	2.052(4)	O(6)#2−Fe(1)−O(2)	88.60(17)
Fe(2)−O(1)	1.905(6)	O(6)#2−Fe(1)−O(7)#3	88.79(17)
Fe(2)−O(3)	1.997(4)	O(6)#2−Fe(1)−N(3)	85.8(2)
Fe(2)−O(4)#1	2.003(5)	O(7)#3−Fe(1)−N(3)	84.06(19)
Fe(2)−N(1)	2.044(8)	O(1)−Fe(2)−O(3)#4	92.97(14)
O(1)−Fe(1)#4	1.914(3)	O(1)−Fe(2)−O(4)#1	94.83(14)
O(5)−Fe(1)#6	2.016(4)	O(1)−Fe(2)−N(1)	180.0(5)
O(6)−Fe(1)#7	2.018(4)	O(3)−Fe(2)−O(3)#4	174.1(3)
O(7)−Fe(1)#8	2.052(4)	O(3)−Fe(2)−O(4)#1	90.90(18)
O(1)−Fe(1)−O(2)	96.96(17)	O(3)#4−Fe(2)−O(4)#1	88.60(18)
O(1)−Fe(1)−O(5)#1	94.72(16)	O(3)#4−Fe(2)−N(1)	87.03(14)
O(1)−Fe(1)−O(6)#2	94.08(15)	O(4)#5−Fe(2)−O(4)#1	170.3(3)
O(1)−Fe(1)−O(7)#3	93.66(17)	O(4)#5−Fe(2)−N(1)	85.17(14)
O(1)−Fe(1)−N(3)	177.7(2)	Fe(1)#4−O(1)−Fe(1)	121.1(3)
O(2)−Fe(1)−O(7)#3	169.22(17)	Fe(2)−O(1)−Fe(1)	119.45(15)
O(2)−Fe(1)−N(3)	85.32(19)	Fe(2)−O(1)−Fe(1)#4	119.45(15)

Symmetry transformations used to generate equivalent atoms: #1 = − y + 1/3, − x + 2/3, z + 1/6, #2 = y, − x + y, − z; #3 = − x + y + 1/3, y − 1/3, z + 1/6; #4 = y + 1/3, x − 1/3, − z + 1/6; #5 = − x + 1, − y, −z; #6 = − y + 2/3, − x + 1/3, z − 1/6; #7 = x − y, x, −z; #8 = − x + y + 2/3, y + 1/3, z −1/6.

Supplementary References

(1) Dziobkowski, C. T.; Wrobleski, J. T.; Brown, D. B. *Inorg. Chem.* **1981**, *20*, 679.

(2) (a) Sheldrick, G. M. *A short history of SHELX*; Society of St. John the Evangelist, Desclée, **1955**. (b) Sheldrick; George, M. *Acta Cryst.* **2001**, *71*, 3.

(3) Dolomanov, O. V.; Bourhis, L. J.; Gildea, R. J.; Howard, J. A. K.; Puschmann, H. *J. Appl. Crystallogr.* **2001**, *42*, 339.

(4) (a) Spek, A. L. *J. Appl. Crystallogr.* **2003**, *36*, 7. (b) Wang, X.-F.; Zhang, Y.-B.; Huang, H.; Zhang, J.-P.; Chen, X.-M. *Cryst. Growth Des.* **2008**, *8*, 4559.

(5) Alexandrov, E. V.; Blatov, V. A.; Kochetkov, A. V.; Proserpio, D. M. *CrystEngComm* **2011**, *13*, 3947.

(6) (a) Lee, C.; Yang, W.; Parr, R. G. *Phys. Rev. B: Condens. Matter Mater. Phys.* **1988**, *37*, 785. (b) Becke, A. D. *J. Chem. Phys.* **1993**, *98*, 5648.

(7) P. J. Hay and W. R. Wadt, *J. Chem. Phys.* **1985**, *82*, 270.

(8) Dolg, M.; Wedig, U.; Stoll, H.; Preuss, H. *J. Chem. Phys.* **1987**, *86*, 866.

(9) (a) Barone, V.; Cossi, M. *J. Phys. Chem. A* **1998**, *102*, 1995. (b) Cossi, M.; Rega, N.; Scalmani, G.; Barone, V. *J. Comput. Chem.* **2003**, *24*, 669. (c) Tomasi, J.; Mennucci, B.; Cammi, R. *Chem. Rev.* **2005**, *105*, 2999.

(10) Gaussian 09, Revision D.01, Frisch, M. J.; Trucks, G. W.; Schlegel, H. B.; Scuseria, G. E.; Robb, M. A.; Cheeseman, J. R.; Scalmani, G.; Barone, V.; Mennucci, B.; Petersson, G. A.; Nakatsuji, H.; Caricato, M.; Li, X.; Hratchian, H. P.; Izmaylov, A. F.; Bloino, J.; Zheng, G.; Sonnenberg, J. L.; Hada, M.; Ehara, M.; Toyota, K.; Fukuda, R.; Hasegawa, J.; Ishida, M.; Nakajima, T.; Honda, Y.; Kitao, O.; Nakai, H.; Vreven, T.; Montgomery, J. A., Jr.; Peralta, J. E.; Ogliaro, F.; Bearpark, M.; Heyd, J. J.; Brothers, E.; Kudin, K. N.; Staroverov, V. N.; Kobayashi, R.; Normand, J.; Raghavachari, K.; Rendell, A.; Burant, J. C.; Iyengar, S. S.; Tomasi, J.; Cossi, M.; Rega, N.; Millam, J. M.; Klene, M.; Knox, J. E.; Cross, J. B.; Bakken, V.; Adamo, C.; Jaramillo, J.; Gomperts, R.; Stratmann, R. E.; Yazyev, O.; Austin, A. J.; Cammi, R.; Pomelli, C.; Ochterski, J. W.; Martin, R. L.; Morokuma, K.; Zakrzewski, V. G.; Voth, G. A.; Salvador, P.; Dannenberg, J. J.; Dapprich, S.; Daniels, A. D.; Farkas, Ö.; Foresman, J. B.; Ortiz, J. V.; Cioslowski, J.; Fox, D. J. Gaussian, Inc., Wallingford CT, **2009**.

(11) Slade, R. C. T.; Hardwick, A.; Dickens, P. G. *Solid State Ionics* **1983**, *s9–10*, 1093.

(12) Yamada, T.; Sadakiyo, M.; Kitagawa, H. *J. Am. Chem. Soc.* **2015**, *131*, 3144.

(13) Taylor, J. M.; Mah, R. K.; Moudrakovski, I. L.; Ratcliffe, C. I.; Vaidhyanathan, R.; Shimizu, G. K. H. *J. Am. Chem. Soc.* **2010**, *132*, 14055.

(14) Pardo, E.; Train, C.; Gontard, G.; Boubekeur, K.; Fabelo, O.; Liu, H.; Dkhil, B.; Lloret, F.; Nakagawa, K.; Tokoro, H. *J. Am. Chem. Soc.* **2011**, *133*, 15328.

(15) Shigematsu, A.; Yamada, T.; Kitagawa, H. *J. Am. Chem. Soc.* **2011**, *133*, 2034.

(16) Dey, C.; Kundu, T.; Banerjee, R. *Chem. Commun.* **2012**, *48*, 266.

(17) Sadakiyo, M.; Okawa, H.; Shigematsu, A.; Ohba, M.; Yamada, T.; Kitagawa, H. *J. Am. Chem. Soc.* **2012**, *134*, 5472.

(18) Kundu, T.; Sahoo, S. C.; Banerjee, R. *Chem. Commun.* **2012**, *48*, 4998.

(19) Panda, T.; Kundu, T.; Banerjee, R. *Chem. Commun.* **2013**, *49*, 6197.

(20) Taylor, J. M.; Dawson, K. W.; Shimizu, G. K. H. *J. Am. Chem. Soc.* **2013**, *135*, 1193.

(21) Wei, M. L.; Wang, X. X.; Duan, X. Y. *Chem-Eur. J.* **2013**, *19*, 1607.

(22) Liang, X.; Zhang, F.; Feng, W.; Zou, X.; Zhao, C.; Na, H.; Liu, C.; Sun, F.; Zhu, G.

Chem. Sci. **2013**, *4*, 983.

(23) Wei, M.; Wang, X.; Sun, J.; Duan, X. *J. Solid State Chem.* **2013**, *202*, 200.

(24) Dong, X. Y.; Wang, R.; Li, J. B.; Zang, S. Q.; Hou, H. W.; Mak, T. C. *Chem. Commun.* **2013**, *49*, 10590.

(25) Kim, S. R.; Dawson, K. W.; Gelfand, B. S.; Taylor, J. M.; Shimizu, G. K. H. *J. Am. Chem. Soc.* **2013**, *135*, 963.

(26) Nagarkar, S. S.; Unni, S. M.; Sharma, A.; Kurungot, S.; Ghosh, S. K. *Angew. Chem. Int. Ed.* **2014**, *53*, 2638.

(27) Zhu, M.; Hao, Z. M.; Song, X. Z.; Meng, X.; Zhao, S. N.; Song, S. Y.; Zhang, H. J. *Chem. Commun.* **2014**, *50*, 1912.

(28) Liu, Y.; Yang, X.; Miao, J.; Tang, Q.; Liu, S.; Shi, Z.; Liu, S. *Chem. Commun.* **2014**, *50*, 10023.

(29) Sadakiyo, M.; Yamada, T.; Honda, K.; Matsui, H.; Kitagawa, H. *J. Am. Chem. Soc.* **2014**, *136*, 7701.

(30) Ju, P. W.; Ram, L. W.; Kicheon, Y.; Won, R. D.; Bongsoo, K.; Hong, C. S. *Angew. Chem. Int. Ed.* **2014**, *53*, 8383.

(31) Wei, M. L.; Sun, J. J.; Duan, X. Y. *Eur. J. Inorg. Chem.* **2014**, *2014*, 345.

(32) Bao, S. S.; Otsubo, K.; Taylor, J. M.; Jiang, Z.; Zheng, L. M.; Kitagawa, H. *J. Am. Chem. Soc.* **2014**, *136*, 9292.

(33) Jiao, Y. Q.; Zang, H. Y.; Wang, X. L.; Zhou, E. L.; Song, B. Q.; Wang, C. G.; Shao, K. Z.; Su, Z. M. *Chem. Commun.* **2015**, *51*, 11313.

(34) Zhao, S. N.; Song, X. Z.; Zhu, M.; Meng, X.; Wu, L. L.; Song, S. Y.; Wang, C.; Zhang, H. J. *Dalton Trans.* **2014**, *44*, 948.

(35) Li, X.; Sun, X.; Li, X.; Fu, Z.; Su, Y.; Xu, G. *Cryst. Growth Des.* **2015**, *15*, 4543.

(36) Barbosa, P.; Rosero-Navarro, N. C.; Shi, F. N.; Figueiredo, F. M. L. *Electrochim. Acta* **2015**, *153*, 19.

(37) Ramaswamy, P.; Wong, N. E.; Gelfand, B. S.; Shimizu, G. K. H. *J. Am. Chem. Soc.* **2015**, *137*, 7640.

(38) Sanda, S.; Biswas, S.; Konar, S. *Inorg. Chem.* **2015**, *54*, 1218.

(39) Meng, X.; Song, S. Y.; Song, X. Z.; Zhu, M.; Zhao, S. N.; Wu, L. L.; Zhang, H. J. *Chem. Commun.* **2015**, *51*, 8150.

(40) Phang, W. J.; Jo, H.; Lee, W. R.; Song, J. H.; Yoo, K.; Kim, B. S.; Hong, C. S. *Angew. Chem. Int. Ed.* **2015**, *54*, 5142.

(41) Borges, D. D.; Devautour-Vinot, S.; Jobic, H.; Ollivier, J.; Nouar, F.; Semino, R.; Devic, T.; Serre, C.; Paesani, F.; Maurin, G. *Angew. Chem. Int. Ed.* **2016**, *128*, 3987.

(42) Li, C.; Sun, M.; Xu, L.; Wang, Y.; Huang, J. *CrystEngComm* **2016**, *18*, 596.

(43) Tu, T. N.; Phan, N. Q.; Vu, T. T.; Nguyen, H. L.; Cordova, K. E.; Furukawa, H. *J. Mater. Chem. A* **2016**, *4*, 3638.

(44) Pili, S.; Argent, S. P.; Morris, C. G.; Rought, P.; Garcíasakai, V.; Silverwood, I. P.; Easun, T. L.; Ming, L.; Warren, M. R.; Murray, C. A. *J. Am. Chem. Soc.* **2016**, *138*, 6352.

(45) Nguyen, N. T. T.; Furukawa, H.; Gándara, F.; Trickett, C. A.; Jeong, H. M.; Cordova, K. E.; Yaghi, O. M. *J. Am. Chem. Soc.* **2015**, *137*, 15394.